

O.O. Grygorenko, K.V. Popiuk, V.V. Kuryliuk

## **Phonon thermal conductivity of nanograined zirconium diboride: molecular dynamics study**

*Taras Shevchenko National University of Kyiv, Faculty of Physics, Kyiv, Ukraine, [kuryliuk@knu.ua](mailto:kuryliuk@knu.ua)*

In this study, the characteristics of phonon transport in single-crystal and nanograined zirconium diboride have been examined using the molecular dynamics method. In the case of single-crystal  $\text{ZrB}_2$  the anisotropy of the phonon thermal conductivity decreased gradually with increasing temperature. The results demonstrate that a reduction in grain size in nanograined  $\text{ZrB}_2$  leads to a decline in thermal conductivity. At a grain size of 1 nm, further reduction does not affect the thermal conductivity of the material. The findings are explained in terms of the scattering of heat carriers at the interfaces and the amorphization of the grain structure.

**Keywords:** zirconium diboride, ceramic, nanograined, thermal conductivity, molecular dynamics.

Received 24 October 2024; Accepted 28 October 2025.

### **Introduction**

Zirconium diboride ( $\text{ZrB}_2$ ) is considered an ultra-high temperature structural material with an unusual combination of properties, including a high melting point (3245 °C) [1], hardness of few tens of GPa [2], appreciable electrical conductivity ( $9.2 \times 10^{-6} \Omega \cdot \text{cm}$ ), and good corrosion resistance [3], [4]. Moreover, due to a high thermal conductivity ( $60\text{--}140 \text{ W} \cdot \text{m}^{-1} \cdot \text{K}^{-1}$ ) [5],  $\text{ZrB}_2$  is therefore widely used in various applications involving extremely high-temperature environments, such as leading/trailing edges of hypersonic [6], atmospheric re-entry vehicles [7], and refractory crucibles [1]. In these applications, high thermal conductivity is required to dissipate the heat released due to atmospheric friction [8]. In addition, the high thermal conductivity of the material also contributes to thermal shock resistance [9] and, therefore, increases stability. Thus, fully exploiting thermal transport in ultra-high temperature ceramics is of great importance to advance them in those above applications.

Despite the development of ceramics based on  $\text{ZrB}_2$  for use in high-temperature conditions, the thermal properties of zirconium diboride have not been widely studied to date. Several experimental studies on the thermal conductivity of  $\text{ZrB}_2$  are found in the literature [9–

11]. The  $\text{ZrB}_2$  bond combines covalent, ionic, and metallic bonds. Accordingly, the total thermal conductivity  $k_{tot}$  includes significant phononic ( $k_p$ ) and electronic ( $k_e$ ) contributions. The electronic component  $k_e$  can be estimated by electrical conductivity using the Weidemann-Franz empirical relationship. In contrast, the phononic component  $k_p$  cannot be measured directly, so it is usually obtained by subtracting  $k_e$  from  $k_{tot}$ . For example, Zhang et al. [9] measured both thermal conductivity and electrical conductivity and then estimated the electron and phonon contribution to thermal transport. Thompson et al. [10] showed that the phononic component for  $\text{ZrB}_2$  was less than approximately  $12 \text{ W} \cdot \text{m}^{-1} \cdot \text{K}^{-1}$  at room temperature and concluded that electrons were the dominant thermal carriers. Simultaneously, Zimmermann and co-workers [11] found that  $k_p$  was as high as  $24 \text{ W} \cdot \text{m}^{-1} \cdot \text{K}^{-1}$  below 200°C. Accordingly, the question of the phonon contribution to the thermal conductivity of transition metal diborides remains unresolved, and further study is necessary to address it.

Due to the challenges in experiments, computer modeling, including molecular dynamics, as an alternative to understanding thermal transport becomes important. From the computational perspective, Lawson et al. [12] employed the Green-Kubo equilibrium molecular

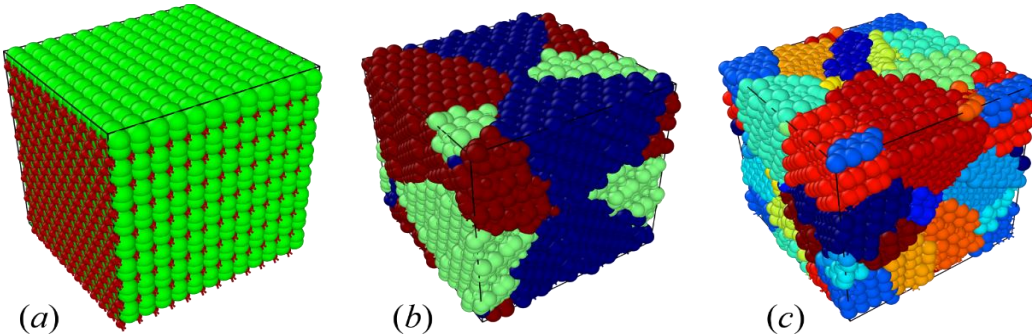


**Fig. 1.** Atomic configurations of the modeled samples: (a) - single crystalline ZrB<sub>2</sub>; (b), (c) - nanograined ZrB<sub>2</sub> with different number of grains. In Fig. (a), zirconium atoms are marked in green, boron atoms are brown. In Figs. (b) and (c), the color of the atoms corresponds to different grains.

dynamics with Tersoff empirical potential to directly estimate the phonon thermal conductivity of ZrB<sub>2</sub>. Their findings revealed a strong correlation with experimental observations [13] within the room temperature range. Simultaneously, some discrepancy was observed in the high-temperature regime, exceeding 1000°C. However, the number of simulation studies investigating heat transport in ceramic materials, including ZrB<sub>2</sub>, is relatively small, mainly due to the lack of a comprehensive database of interatomic potentials.

In this study, we employ the molecular dynamics method to determine the phonon thermal conductivity of ZrB<sub>2</sub>. We first carry out the calculation on the single-crystalline ZrB<sub>2</sub> by considering both in-plane and out-plane phonon transport. The temperature dependencies of thermal conductivity are calculated. Then, the effect of grain size on phonon thermal conductivity in nanograined zirconium diboride is elaborated.

## I. Simulation details

Using LAMMPS (Large-scale Atomic/Molecular Massively Parallel Simulator) software packages [14], molecular dynamics simulations of thermal transport in ZrB<sub>2</sub> samples were performed. The single-crystalline ZrB<sub>2</sub> structure was generated using a primitive hexagonal (AlB<sub>2</sub>-type, P6/mmm space group) lattice with nominal lattice constants  $a = 3.17$  Å and  $c = 3.53$  Å [1]. This supercell was then replicated in the three spatial directions (Figure 1, a), resulting in a ZrB<sub>2</sub> box containing about  $2.5 \cdot 10^4$  atoms. The nanograined ZrB<sub>2</sub> samples were generated using the three-dimensional Voronoi construction method [15]. In this method, a set of randomly distributed seed points defines the grain centers, and the simulation cell is partitioned into convex polyhedra (Voronoi cells) such that each region contains all points closest to a given seed. Each grain is then assigned a random crystallographic orientation, and atoms are placed accordingly to form grain boundaries representative of realistic nanocrystalline structures. Several atomistic models with a various mean grain sizes were developed in this study (Figure 1, b, c). The grain sizes and orientations were randomly determined using a Voronoi tessellation. In our study, the grain size for each nanograined model was defined as the average equivalent spherical diameter of grains, calculated from the Voronoi

tessellation.

The initial velocities of atoms were sampled in accordance with Maxwell distribution. The velocities and positions of atoms along with the simulations were solved by using Verlet velocity algorithm. The empirical Tersoff force field was performed, of which rigorous force field parameters were obtained by utilizing high level first principles.

The obtained conformations of the nanograined ZrB<sub>2</sub> samples were unstable and unreasonable due to their non-minimal potential energy. Thus the energy minimization treatment, adopting conjugate gradient method, should be carried out to search minimal potential energy of the systems. Then, the structures were relaxed under the NPT and NVT ensembles, respectively for 100 ps.

The thermal conductivity was determined using a non-equilibrium molecular dynamics method based on the Müller-Plathe algorithm [16]. In this approach, the sample was divided into thin slabs along the direction of calculation, as illustrated in Figure 2, a. At 500-timestep intervals throughout the dynamics process, kinetic energy was swapped between the slowest atom in the central layer and the highest one in the edge layer [17]. This process is equivalent to the appearance of heat flow  $q$ . As a result of the interaction between atoms from neighbouring layers, a stationary temperature gradient is established within the system over time. The energy cost of each swap and the temperature gradient are recorded, enabling the determination of the thermal conductivity  $k$  using the following equation [18]:

$$k = -\frac{q}{dT/dz} \quad (1)$$

In order to obtain the temperature gradient  $dT/dz$  for each temperature profile, as illustrated in Figure 2,a, a linear fitting to the data within an appropriate range is conducted. The slopes of the two fitted lines are averaged, and the resulting value is defined as the temperature gradient. The non-equilibrium molecular dynamics simulations at different temperature were performed after obtaining a reasonable initial structures. Temperature within range from 300 K to 1500 K was controlled by Nose-Hoover method. The simulation time is 2000 ps with time step of 1 fs.

It is worth noting that the thermal conductivity values obtained by nonequilibrium molecular dynamics can be sensitive to the size of the simulated cell. However, in

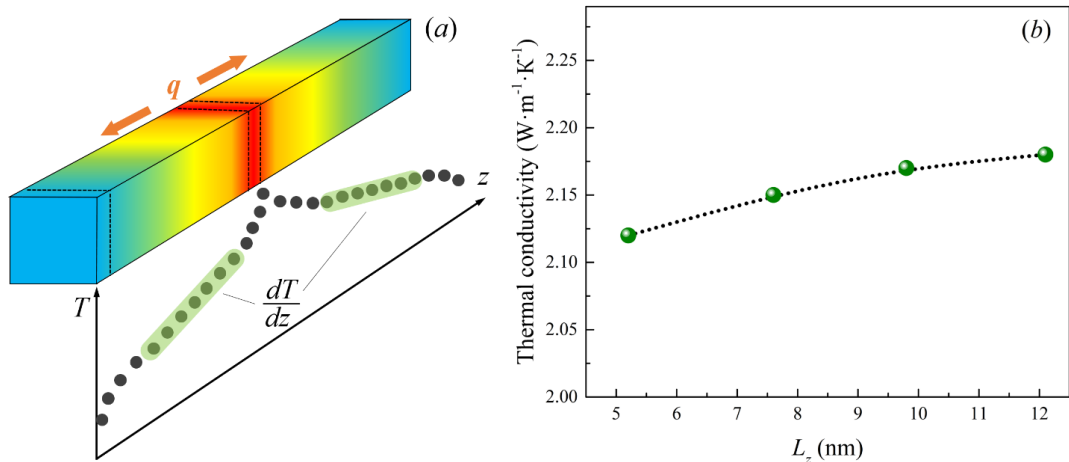


**Fig. 2.** (a) - Schematic model for non-equilibrium molecular dynamics simulations. A small amount of heat is repeatedly added into the hot region (red color) and removed from the cold regions (blue color) to create the heat fluxes from the hot region to the cold region. Typical temperature profile along the heat flux direction is shown at the bottom of the figure. The temperature gradient is extracted from the linear portions highlighted by the green lines. (b) - Effect of  $L_z$  size on the thermal conductivity of nanocrystalline zirconium diboride.

structures where the phonon mean free path is strongly limited and does not exceed the cell dimensions, this size effect becomes negligible. The nanocrystalline zirconium diboride structures studied here are examples of systems with significantly restricted phonon transport due to the extensive grain boundary area, allowing the size effect to be disregarded in our simulations. To illustrate this, Fig. 2, b shows the calculated dependence of thermal conductivity on the  $L_z$  dimension (with the other two dimensions kept constant) for one of the nanocrystalline samples. It is easy to see that with an increase of  $L_z$  almost twofold, the change in the thermal conductivity coefficient does not exceed 4%.

## II. Results and discussions

To verify that the presented model works correctly, we first conducted simulations of the temperature dependence of the phonon thermal conductivity for single-crystalline  $\text{ZrB}_2$ . The bulk thermal conductivities of zirconium diboride for both in-plane and out-plane directions at different temperatures are shown in Figure 3. It is known that the thermal conductivity mainly depends on the mean free path of phonons. So, when the temperature is increased, the thermal vibrations of particles are enhanced, and the mean free path of phonons is reduced. Therefore, the thermal conductivity of the single-crystalline  $\text{ZrB}_2$  sample is decreased with the increase in temperature, as can be seen from Figure 3.

At room temperature, the in-plane thermal conductivity  $k_{in}$  exceeded the out-of-plane value  $k_{out}$ . This phenomenon may be attributed to the contribution of phonon scattering at the boundaries between the Zr and B layers, which facilitates thermal transport in addition to the phonon-phonon scattering mechanism. At higher temperatures, the difference between the in-plane and out-plane thermal conductivities is negligible, and  $k_{in} \approx k_{out}$  above  $T \sim 1000$  K. The results demonstrate that at temperatures exceeding 1000 K, phonon-phonon scattering assumes a dominant role in both directions of

heat propagation, while the impact of interfacial boundaries on thermal transport becomes nearly undetectable. It is noteworthy that the dependencies illustrated in Figure 3 exhibit a strong correlation with the findings of the referenced work [12], thereby demonstrating the efficacy of the presented model in accurately predicting the thermal conductivities of nanograined zirconium diboride.

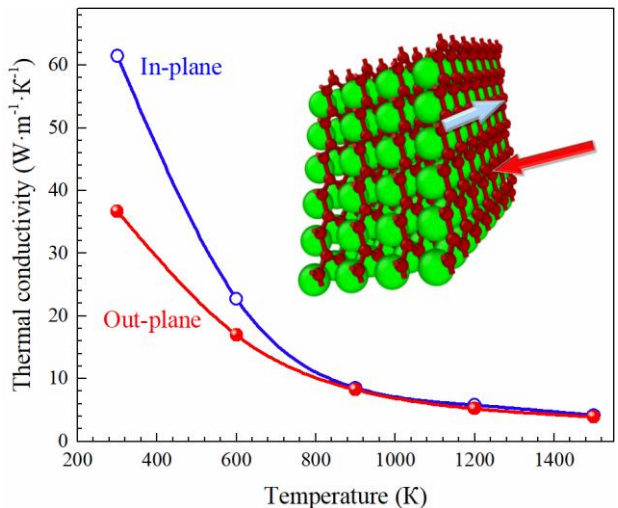


**Fig. 3.** Thermal conductivity of the single-crystalline  $\text{ZrB}_2$  as a function of temperature.

Next, the thermal conductivity of nanograined  $\text{ZrB}_2$  was examined using non-equilibrium molecular dynamics. Figure 4 shows the results for three  $\text{ZrB}_2$  samples with different grain sizes  $D$ . It can be observed that the temperature dependence of the thermal conductivity of zirconium diboride undergoes a change with the variation of grain size. In particular, as the grain size decreases, the rate of decrease in thermal conductivity with increasing temperature also decreases. Furthermore, for samples with grains whose size is less than  $D=1$  nm, the thermal conductivity practically ceases to depend on temperature. This change in the  $k(T)$  dependence is the result of two main factors. First, as grain size decreases,

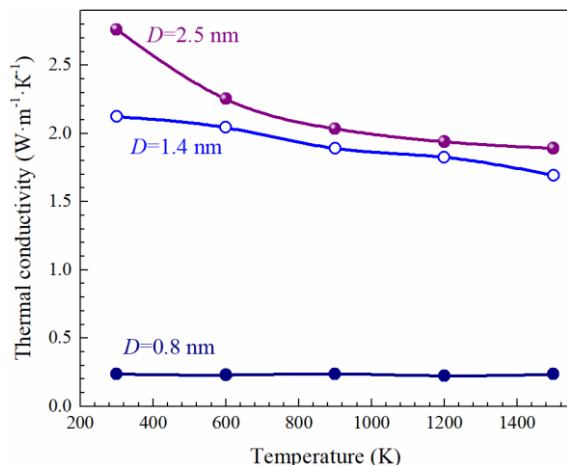


**Fig. 4.** Thermal conductivity of the nanograin ZrB<sub>2</sub> with different grain sizes as a function of temperature.

the area of intergranular boundaries increases, resulting in an increase in the rate of thermal oscillation dissipation. Second, small grains can undergo structural changes due to the rearrangement of atoms, leading to a violation of the crystal structure with a corresponding decrease in thermal conductivity. A similar effect has been studied for other types of nanostructures [19].

In addition, Figure 4 shows that a decrease in grain size leads to a decrease in the thermal conductivity in the studied temperature range. The corresponding dependence of thermal conductivity on grain size at  $T = 300$  K is shown in Figure 5. It is noticeable that the decrease in thermal conductivity occurs approximately up to a grain size of about 1 nm. For smaller sizes, the thermal conductivity coefficient practically does not change and is equal to  $0.3 \text{ W}\cdot\text{m}^{-1}\cdot\text{K}^{-1}$ . This result confirms the above considerations about the structural rearrangement of the material. In fact, the evaluation shows that at a grain size of about 1 nm, the proportion of atoms on the grain surface exceeds 70%. This leads to a large number of unfilled bonds in the structure and thus to an increase in the average energy. To minimize it, surface atoms are rearranged, resulting in significant changes in the material structure, including the formation of amorphized regions. And it is the amorphization of grains at  $D < 1$  nm that makes the phonon thermal conductivity of nanograin ZrB<sub>2</sub> independent of temperature.

## Conclusions

In the present study, molecular dynamics simulations

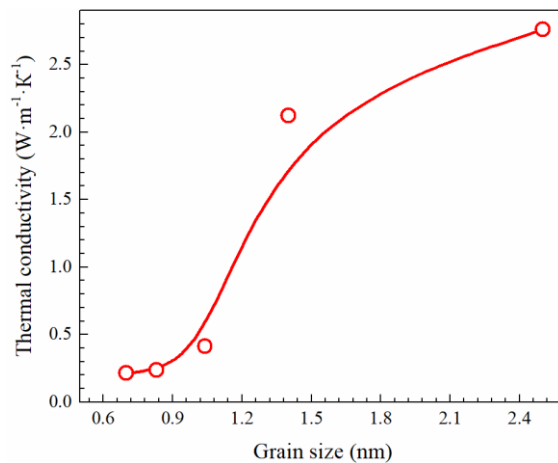


**Fig. 5.** Thermal conductivity of nanograin ZrB<sub>2</sub> as a function of grain size at  $T = 300$  K.

of phonon heat transport in zirconium diboride have been conducted. The results demonstrate that at room temperature, the thermal conductivity of single-crystal ZrB<sub>2</sub> in the direction parallel to the Zr and B layers is approximately twice as high as in the perpendicular direction. The findings revealed a decline in the thermal conductivity of nanograin zirconium diboride with a reduction in grain size. At average grain sizes below 1 nm, the thermal conductivity exhibits a pronounced decline and becomes independent of temperature and grain size. The sharp decrease in the thermal conductivity of nanograin ZrB<sub>2</sub> with grains smaller than 1 nm may be attributed to the prevalence of phonon scattering at the grain boundaries and the concurrent amorphization of the structure due to a substantial proportion of atoms on the surface and their rearrangement.

## Acknowledgments

This work was supported by the National Research Foundation of Ukraine (Project No 2023.04/0139). The authors would like to acknowledge the use of computational resources provided by the SKIT computing cluster of the Glushkov Institute of Cybernetics of the National Academy of Sciences of Ukraine.

**Grygorenko O.O.** – Student of the Department of Metal Physics.

**Popiuk K.V.** - Student of the Department of Metal Physics.

**Kuryliuk V.V.** - Candidate of Physical and Mathematical Sciences (PhD), Head of the Department of Metal Physics.

- [1] W.G. Fahrenholtz, G.E. Hilmas, J. Am. Ceram. Soc., *Refractory diborides of zirconium and hafnium* 90(5) 1347 (2007); <https://doi.org/10.1111/j.1551-2916.2007.01583.x>.
- [2] Z. Wang, C.Q. Hong, X.H. Zhang, X. Sun, J.C. Han, Mater. Chem. Phys., *Microstructure and thermal shock behavior of ZrB<sub>2</sub>–SiC–graphite composite* 113, 338 (2009); <https://doi.org/10.1016/j.matchemphys.2008.07.095>.
- [3] X.H. Zhang, Z. Wang, P. Hu, W.B. Han, C.Q. Hong, Scr. Mater., *Mechanical properties and thermal shock resistance of ZrB<sub>2</sub>–SiC ceramic toughened with graphite flake and SiC whiskers*, 61, 809 (2009); <https://doi.org/10.1016/j.scriptamat.2009.07.001>.
- [4] G.J. Zhang, Y.D. Deng, N. Kondo, J.F. Yang, T. Ohji, J. Am. Ceram. Soc., *Reactive hot pressing of ZrB<sub>2</sub>–SiC composites*, 83 (9), 2330 (2000); <https://doi.org/10.1111/j.1551-2916.2000.tb01558.x>.

- [5] M.M Opeka, I.G. Talmy, E.J. Wuchina, J.A. Zaykoski, S.J. Causey, J. Eur. Ceram. Soc., *Mechanical, thermal, and oxidation properties of refractory hafnium and zirconium compounds* 19(13), 2405 (1999); [https://doi.org/10.1016/S0955-2219\(99\)00129-6](https://doi.org/10.1016/S0955-2219(99)00129-6).
- [6] M.M. Opeka, I.G. Talmy, J.A. Zaykoski, J. Mater. Sci., *Oxidation-based materials selection for 2000 °C + hypersonic aerosurfaces: theoretical considerations and historical experience* 39 (19), 5887 (2004); <https://doi.org/10.1023/b:jmsc.0000041686.21788.77>.
- [7] M.J. Gasch, D.T. Ellerby, S.M. Johnson, *Handbook of ceramic composites, Ultra high temperature ceramic composites* 9, 197 (2005); [http://doi.org/10.1007/0-387-23986-3\\_9](http://doi.org/10.1007/0-387-23986-3_9).
- [8] T.H. Squire, J. Marschall, J. Eur. Ceram. Soc., *Material property requirements for analysis and design of UHTC components in hypersonic applications* 30(11), 2239 (2010); <https://doi.org/10.1016/j.eurceramsoc.2010.01.026>.
- [9] L. Zhang, D.A. Pejakovic', J. Marschall, M. Gasch, J. Am. Ceram. Soc., *Thermal and electrical transport properties of spark plasma-sintered HfB<sub>2</sub> and ZrB<sub>2</sub> ceramics* 94(8), 2562 (2011); <https://doi.org/10.1111/j.1551-2916.2011.04411.x>.
- [10] J. W. Zimmermann, G. E. Hilmas, W. G. Fahrenholtz, R. B. Dinwiddie, W. D. Porter, H. Wang, J. Am. Ceram. Soc, *Thermophysical properties of ZrB<sub>2</sub> and ZrB<sub>2</sub>-SiC ceramics* 91, 1405 (2008); <https://doi.org/10.1111/j.1551-2916.2008.02268.x>.
- [11] M. J. Thompson, W. G. Fahrenholtz, G. E. Hilmas, J. Am. Ceram. Soc, *Elevated temperature thermal properties of ZrB<sub>2</sub> with carbon additions* 95, 1077 (2012); <https://doi.org/10.1111/j.1551-2916.2011.05034.x>.
- [12] J.W. Lawson, M.S. Daw, C.W. Bauschlicher, Jr J. Appl. Phys, *Lattice thermal conductivity of ultra high temperature ceramics ZrB<sub>2</sub> and HfB<sub>2</sub> from atomistic simulations* 110(8), (2011); <http://doi.org/10.1063/1.3647754>
- [13] H. Kinoshita, S. Otani, S. Kamiyama, H. Amano, I. Akasaki, J. Suda, H. Matsunami, Jpn. J. Appl. Phys., *Zirconium Diboride (0001) as an Electrically Conductive Lattice-Matched Substrate for Gallium Nitride* 40 (12A), 1280 (2001); <https://doi.org/10.1143/JJAP.40.L1280>.
- [14] A. P. Thompson, H. M. Aktulga, R. Berger, D. S. Bolintineanu, W. M. Brown, P. S. Crozier, P. J. in 't Veld, A. Kohlmeyer, S. G. Moore, T. D. Nguyen, R. Shan, M. J. Stevens, J. Tranchida, C. Trott, S. J. Plimpton, Comp Phys Comm , *LAMMPS - a flexible simulation tool for particle-based materials modeling at the atomic, meso, and continuum scales* 271, 10817 (2022); <https://doi.org/10.1016/j.cpc.2021.108171>
- [15] J.L Finney, *Journal of Computational Physics*, A procedure for the construction of Voronoi polyhedra, 32, 137-143 (1979); [https://doi.org/10.1016/0021-9991\(79\)90146-3](https://doi.org/10.1016/0021-9991(79)90146-3).
- [16] V.V. Kuryliuk, O.A. Korotchenkov, *Physica E: Low-Dimensional Systems and Nanostructures*, Atomistic simulation of the thermal conductivity in amorphous SiO<sub>2</sub> matrix/Ge nanocrystal composites, 88, 228 (2017); <https://doi.org/10.1016/j.physe.2017.01.021>.
- [17] M. Sanjeeva, M. R. Gilbert, S. T. Murphy, *Fusion Engineering and Design, Molecular dynamics simulations of the effect of porosity on heat transfer in Li<sub>2</sub>TiO<sub>3</sub>202*, 114344 (2024); <https://doi.org/10.1016/j.fusengdes.2024.114344>.
- [18] M. Mansourian-Tabaei, A. Asiaee, B. Hutton-Prager, S. Nouranian, *Applied Surface Science, Thermal barrier coatings for cellulosic substrates: A statistically designed molecular dynamics study of the coating formulation effects on thermal conductivity* 587, 152879 (2022); <https://doi.org/10.1016/j.apsusc.2022.152879>.
- [19] V.V. Kuryliuk, S.S. Semchuk, K.V. Dubyk, R.M. Chornyi, *Nano-Structures and Nano-Objects, Structural features and thermal stability of hollow-core Si nanowires: A molecular dynamic study* 29, 8 (2022); <https://doi.org/10.1016/j.nanoso.2021.100822>.

О.О. Григоренко, К.В. Попюк, В.В. Курилюк

## Фононна тепlopровідність нанозернистого дібориду цирконію: молекулярно-динамічне дослідження

Київський національний університет імені Тараса Шевченка, фізичний факультет, Київ, Україна, [kuryliuk@knu.ua](mailto:kuryliuk@knu.ua)

У цій роботі за допомогою методу молекулярної динаміки досліджено характеристики фононного транспорту в монокристалічному та нанозернистому дібориді цирконію. Виявлено, що у випадку монокристалічного ZrB<sub>2</sub> анізотропія фононної тепlopровідності поступово зменшується з підвищеннем температури. Результати також демонструють, що зменшення розміру зерен у нанозернистому ZrB<sub>2</sub> призводить до зменшення тепlopровідності. При розмірі зерна 1 нм подальше його зменшення не впливає на величину тепlopровідності матеріалу. Отримані результати пояснюються розсіюванням носіїв тепла на границях поділу та аморфізацією зернистої структури.

**Ключові слова:** діборид цирконію, кераміка, нанозернистий, тепlopровідність, молекулярна динаміка.